Examination of a Boundary Layer Jet

MARC E. TOUCHTON

1. Introduction

During the second leg of the OC3570 Oceanography cruise, the R/V Pt Sur experienced strong winds and rough seas August 6-7, 2001. Rawinsondes launched during this period showed the existence of a jet like wind maximum at the boundary layer interface. Also evident from the rawinsonde data was the sloping of the boundary layer from higher heights offshore to lower heights inshore. Just off the coast the weather improved considerably. Winds were light and the seas decreased. Scatterometry data from a pass during the cruise shows the high winds experienced by the ship (Fig. 1).

2. Purpose

The purpose of this project was to examine the boundary layer jet evidenced by the surface and rawinsonde data. Theoretical winds were calculated from the slope of the boundary layer and compared to observed values.

3. Data

The data from the cruise used for this project includes rawinsondes, the quick observations and SAIL data. Three of the rawinsondes from the cruise were during the time period and depict the higher winds at the boundary layer. The locations and time are depicted in Figure 2. The rawinsondes are labeled as Stations 1-3 for the purposes of this project with 1 being the

earliest and 3 the latest. Plots were generated using the downcast portion of the rawinsonde data due to the accuracy of the temperature and dew point calculations being greater. Temperature and dew point from each station are plotted in Figures 3-5. The lower 2000 m of the rawinsondes are plotted with temperature, dew point and wind speeds (Fig. 6-8). Sea surface temperatures were pulled from the Quick observations sheets hand-held IR sensor values. Surface winds were pulled from the SAIL data.

Station 1, the sounding furthest west and south, was omitted for most calculations for a number of reasons. First, the longitudinal proximity to Station 2, but with a much larger height is incongruous. This disparity may have been caused by the heights decreasing in the intervening time and/or the heights also sloped to the south. Unfortunately, insufficient data was collected for the exact reason to be known. Secondly, while Stations 1 and 2 are nearly the same distance off the coast, only Station 2 lines up with Station 3 on a bearing perpendicular to the coast. Finally, Stations 2 and 3 are closer temporally, with approximately 5 hours (5 hr 8 min) between them.

The height of the boundary layer was determined from the rawinsonde height that showed the first significant temperature increase. The heights produced were:

Station 1	Station 2	Station 3
289 m	250 m	225 m

The height of the inversion was determined from the rawinsonde height value where the temperature stopped increasing. The heights obtained were:

Station 1	Station 2	Station 3
637 m	589 m	570 m

These heights were then graphed to depict the slope of the boundary layer and the inversion (Fig. 9). The graph is oriented with Station 3 on the left and Station 2 on the right. It depicts the slope of the layers, as it would be seen looking south. The distance between Stations 2 and 3 was 29.88 km and 30 km was used for ease of calculations. The slope of the boundary layer was 8.33 m per 10 km. The slope of the inversion was 6.33 m per 10 km.

The SST at Station 2 (3) was 16.1 °C (12 °C). The SST temperature gradient was 1.33 °C per 10 km. The surface air temperature at Station 2 (3) was 14.96 °C (13.42 °C). The air temperature gradient at the surface was .5133 °C per 10 km.

Vertical temperature and wind speed profiles were generated between Stations 2 and 3 (Figs. 10 and 11). Temperature and wind speed values were interpolated at every 30 m from the rawinsonde data and then plotted using the contour fill function of MATLAB. These profiles are oriented with Station 3 on the left as in the previous figure. The temperature profile (Fig. 10) shows the sloping gradient associated with the boundary layer. The wind speed profile (Fig. 11) shows the sloping jet core associated with the boundary layer.

4. Dynamics

In geostrophic adjustment, if the Rossby Radius of Deformation squared is less than the length scale squared ($L^2 >> L_R^2$), velocity will adjust to the initial height field. The geostrophic wind can then be calculated using the following formula:

$$Vg = \frac{g}{f} * \frac{\partial H}{\partial x} \quad (1)$$

Where, g is the gravitational constant, 9.8 m s^{-2}, f is the Coriolis force, 10^{-4}, and derivate of H represents the change in height in the x-direction.

In a simple sloping field (Fig. 12), a decreasing slope in the positive y-direction will produce a wind in the negative x-direction or out of the page.

5. Analysis

For the purposes of these calculations, the bearing between Stations 2 and 3 was considered to be in the x-direction, positive in the direction of Station 3. This results in a negative slope value for the boundary layer and the inversion. When calculated using Equation (1), this will result in a negative or northerly wind. The following table shows the calculated geostrophic wind based on the boundary layer slope and the inversion slope between the different stations.

Wind	Stations 1-3	Stations 1-2	Stations 2-3
Boundary	20.9 m/s	17.5 m/s	8.1667 m/s
Inversion	21.8867 m/s	20.6 m/s	6.2067 m/s

The observed winds at the surface, the boundary layer and the inversion at each station are detailed in the following table.

Station	Surface	Boundary Layer	Inversion
1	15 m/s	15 m/s	3.8 m/s
2	11.5 m/s	17 m/s	7.9 m/s
3	9 m/s	13.9 m/s	11.1 m/s

The results computed between Stations 1 and 3 are much higher than any observed values. The slope between these stations is speculated to not be representative of the slope at any time during the cruise. The values between Stations 1 and 2 and Station 2 and 3, however, match the observed values within a safe margin of error. Reasons for the difference will be covered in section 6. Interestingly, the surface wind speed value at Station 3 matches very closely with the calculated geostrophic wind speed for the most representative.

The geostrophic wind calculated should not exactly match the observed values. It does not take into account frictional effects. Nor does it considered the effects of the mean background flow on the wind. Additionally, the value calculated is an average value for the intervening layer and will not necessarily match any of the values recorded by the rawindsonde.

6. Sources of Error

Rawinsonde measurements are very likely the greatest source of errors in the calculations. Wind averaging calculations by the rawinsonde could be in error and do not have enough resolution to clearly describe the wind field. Boundary layer and inversion heights pulled from the rawinsonde data may not

exactly match the actual heights. Wind drift of the sensor could result incorrect distance calculations between the stations at the boundary layer height. The temperature and dew point measurements are also suspect. Any contamination of the sensors could lead to erroneous values.

The temporal and space variations of the rawinsonde measurements also introduce errors to the calculations. A tighter resolution in both space and time would provide more accurate measurement of the variation of the boundary layer height.

Undetected variations of the environment could also lead to incorrect parameterization of the physical characteristics. Once again, a finer resolution of observations would improve the accuracy of the measurements.

Finally, human error in determining the heights, averaging and interpolation of the pertinent values would skew the results.

7. Conclusions

The existence of a jet due to a sloping boundary layer does seem to exist. The limited data collected verifies the slope and the increased winds at the boundary layer. A more detailed study with greater data would define this feature and its characteristics much more adequately.

References

Holton, J. R. An Introduction to Dynamic Meteorology, 3rd Ed. San Diego, 1992.

Class notes from the lectures of Prof. R.T. Williams and R. Haney.

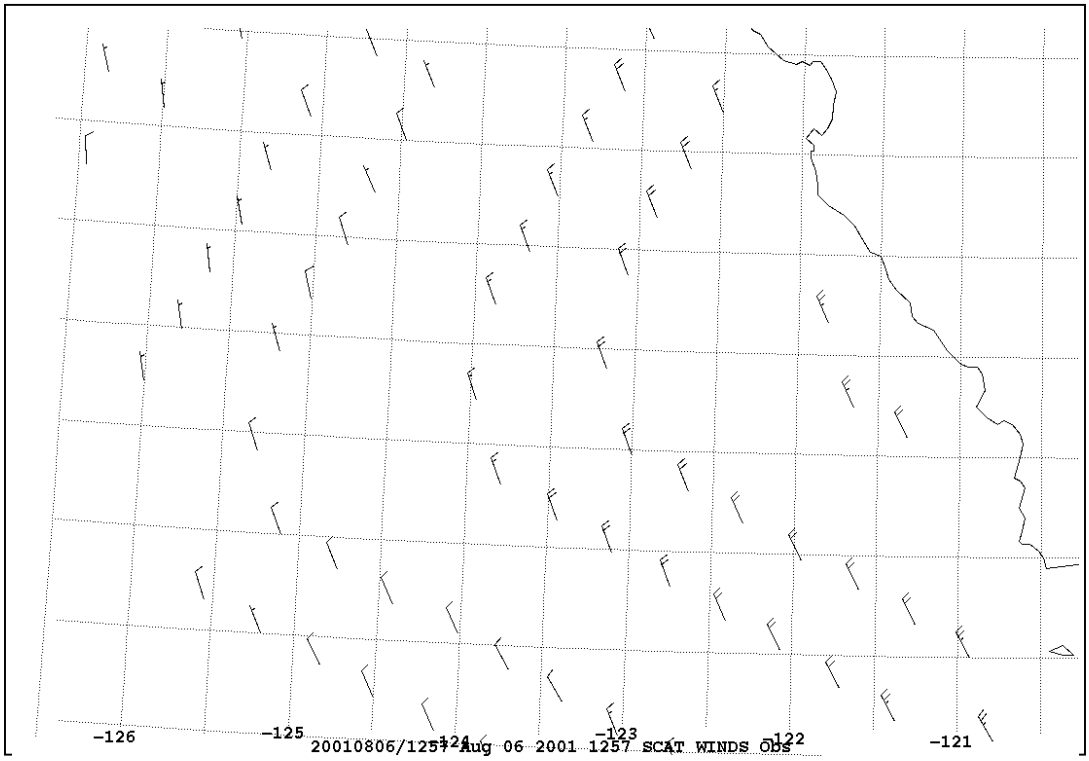

Figure 1. 1257 Aug 06 20001, Scatterometry pass showing the high winds off the California coast for the period of the cruise.

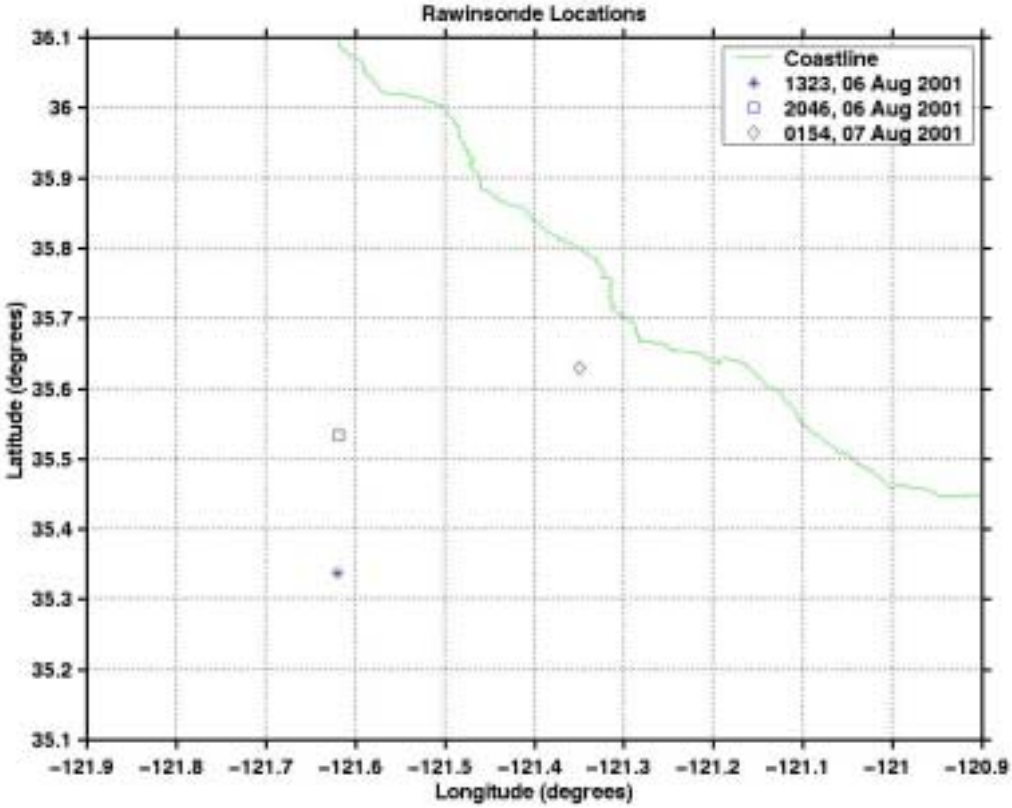

Figure 2. Location and times in GMT of the rawinsonde launches.

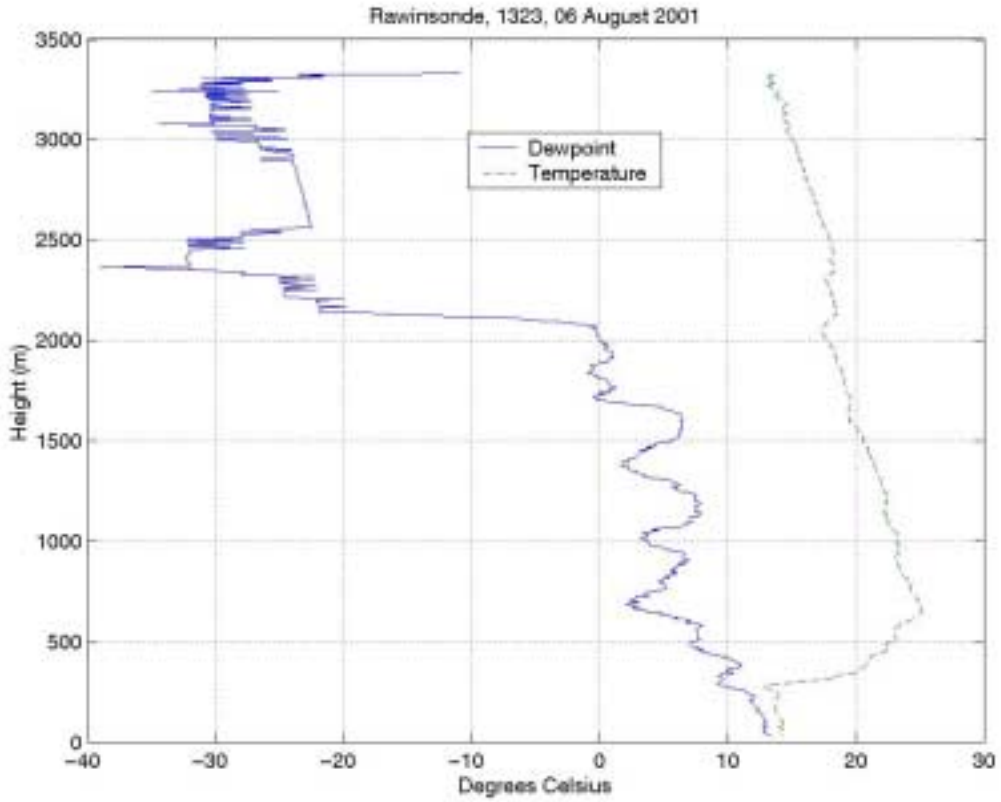

Figure 3. Upper-air sounding taken at 1323 GMT, 06 August 2001, 35 20.25’N 121 37.20’W.

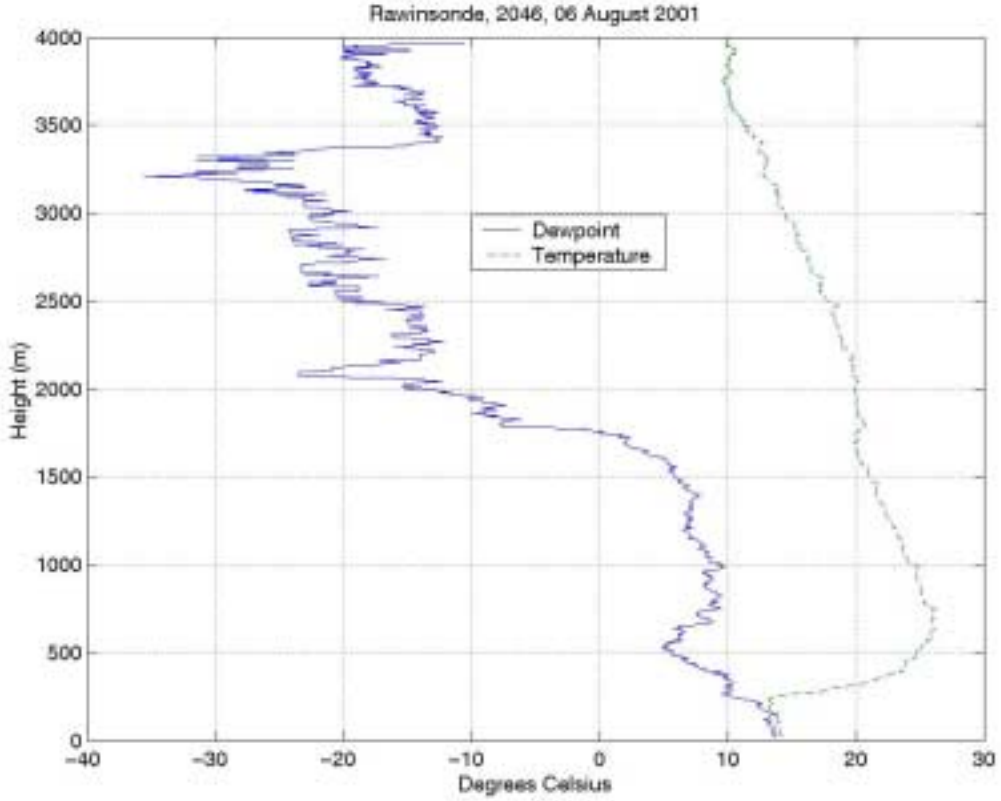

Figure 4. Upper-air sounding taken at 2046 GMT, 06 August 20001, 35 32.019N 121 37.165W.

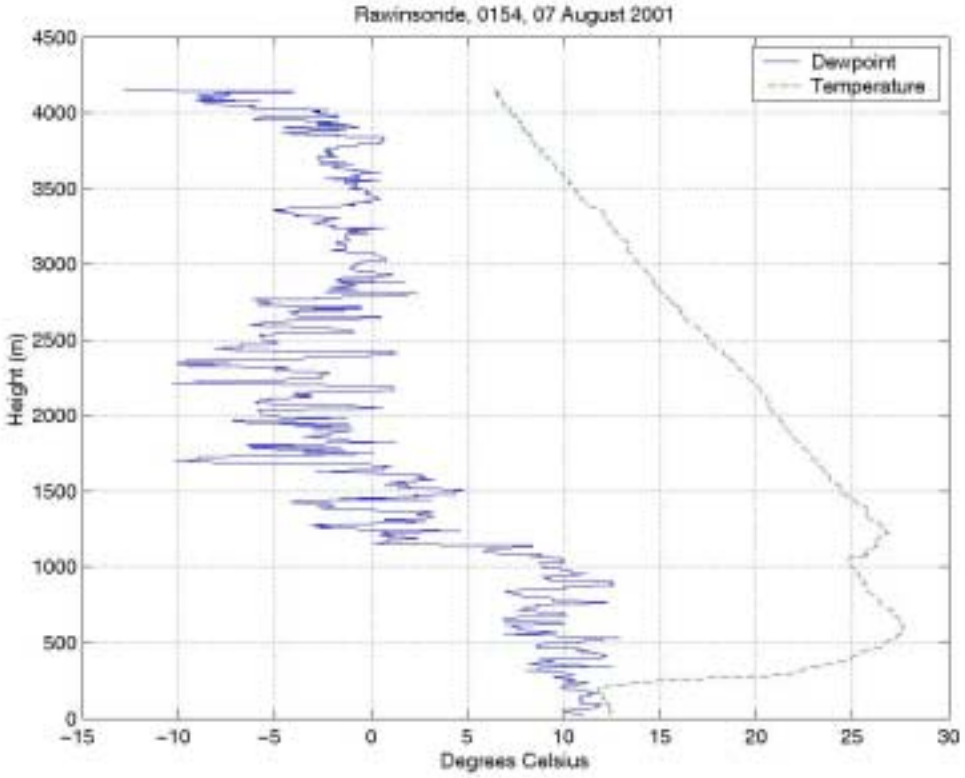

Figure 5. Upper-air sounding taken at 0154, 07 August 2001, 35 37.783N 121 21.01W.

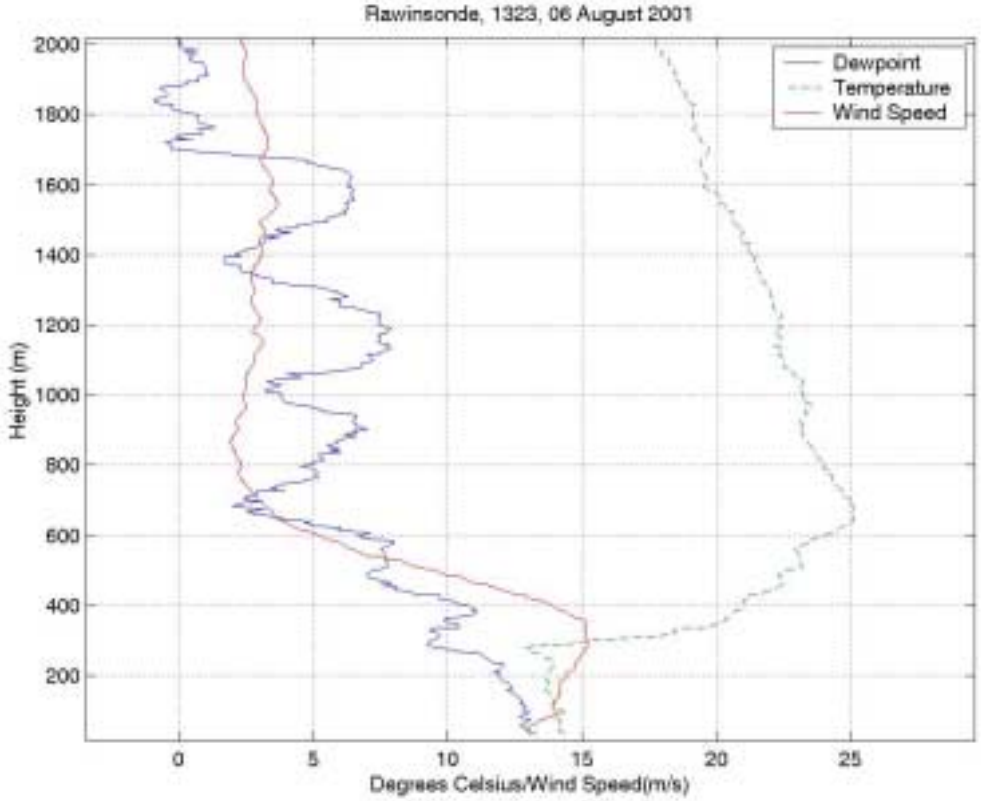

FIG. 6. Lower 2000 m of Station 1 rawinsonde with winds.

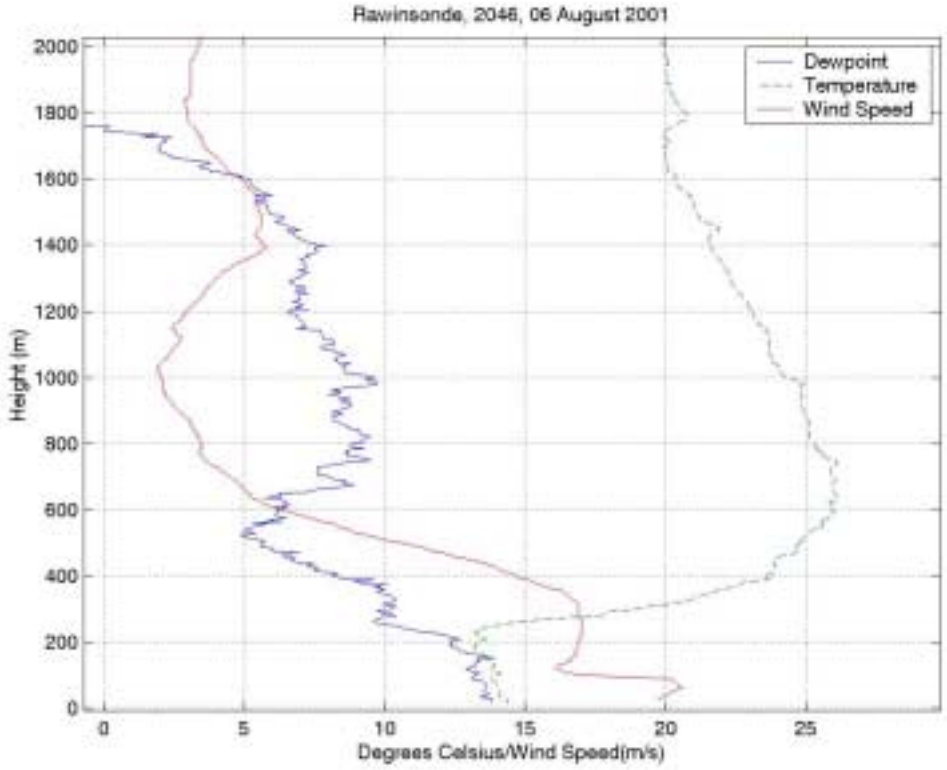

FIG. 7. Lower 2000 m of Station 2 rawinsonde with winds.

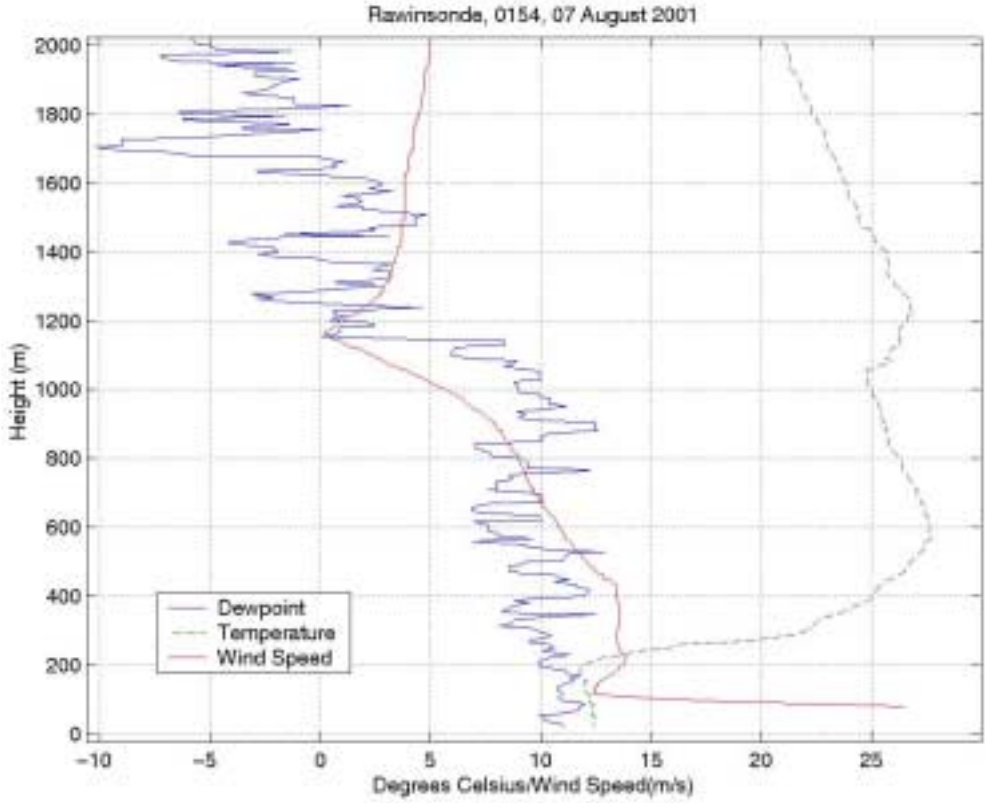

FIG. 8. Lower 2000 m of Station 3 rawinsonde with winds.

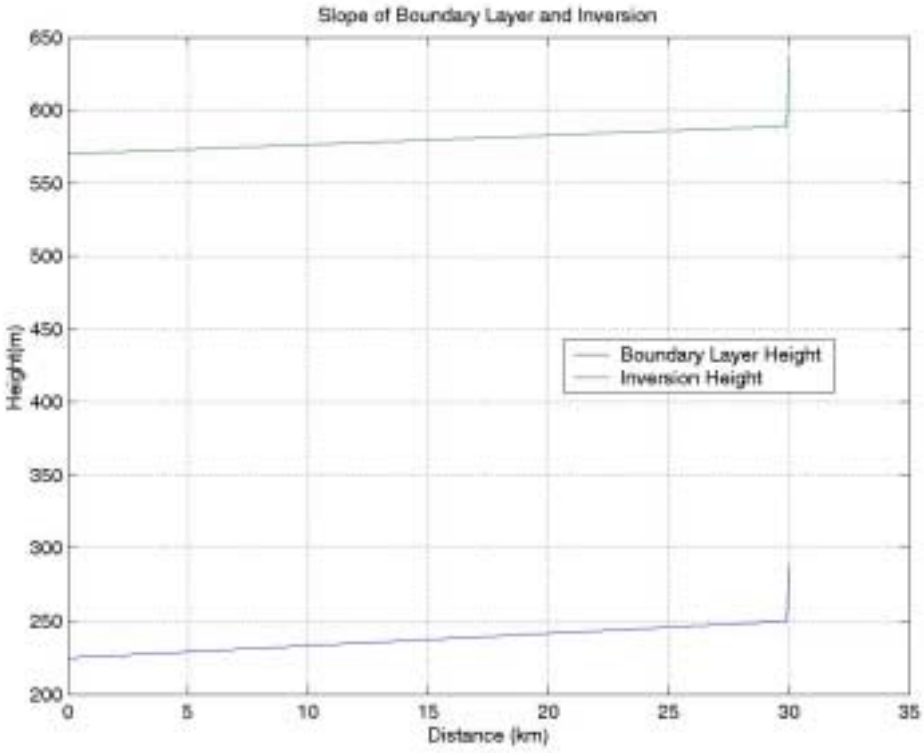

FIG. 9. Boundary layer and inversion heights.

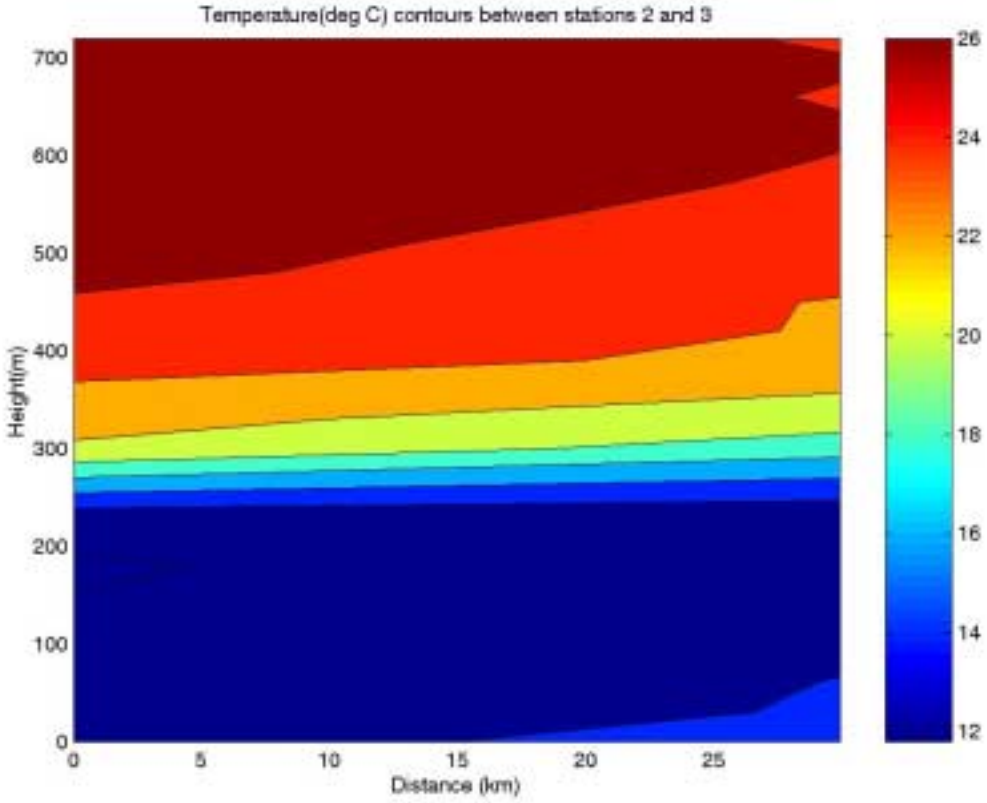

FIG. 10. Temperature profile between Stations 2 and 3.

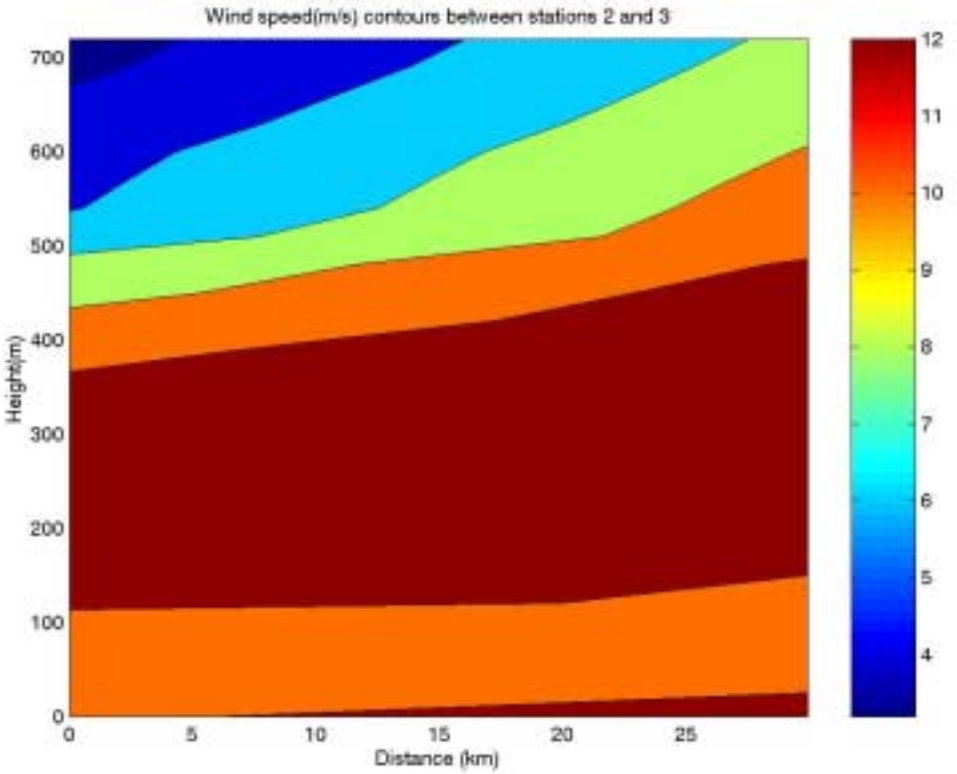

FIG. 11. Wind speed profile between Stations 2 and 3.

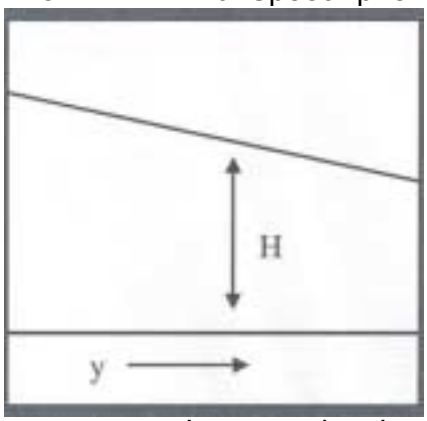

FIG. 12. Diagram showing sloping layer with respect to the y-direction.